OPTICAL ABSORPTION, RAMAN, AND PHOTOLUMINESCENCE EXCITATION SPECTROSCOPY OF INHOMOGENEOUS InGaN FILMS

L.H. Robins,* A.J. Paul,* C.A. Parker,** J.C. Roberts,** S.M. Bedair,**

E.L.Piner,*** N.A. El-Masry***

*National Institute of Standards and Technology (NIST), Gaithersburg, MD 20899
**Electrical and Computer Engineering, North Carolina State University, Raleigh, NC 27695
***Materials Science and Engineering, North Carolina State University, Raleigh, NC 27695

Cite this article as: MRS Internet J. Nitride Semicond. Res. 4S1, G3.22 (1999)

ABSTRACT

$In_xGa_{1-x}N$ films with x=0.06 to x=0.49 were characterized by optical transmittance, Raman, and photoluminescence excitation spectroscopies. Previous microstructural characterizations detected phase separation only in films with x>0.2. The transmittance data suggest that compositional inhomogeneity is also present in the lower-x films (x<0.2). Both Raman and photoluminescence excitation spectra show features that correlate with compositional inhomogeneity and phase separation in the films with x>0.2. The composition dependence of the Raman spectra, from x=0.28 to x=0.49, is consistent with an increase in the size of the phase-separated regions with increasing x.

INTRODUCTION

A new generation of short-wavelength optoelectronic devices is being developed from thin films of the group III nitrides (Al,Ga,In)N. The active layers of visible-emitting devices[1] are usually composed of $In_xGa_{1-x}N$. The growth of $In_xGa_{1-x}N$ layers is complicated by the tendency of GaN-InN alloys to phase separate, which was first observed[2] by Osamura *et. al.* in 1975 with x-ray diffraction (XRD) of annealed polycrystalline samples, and more recently by Singh[3] *et. al.* with XRD and optical absorption, and Piner[4] *et. al.* with XRD, transmission electron microscopy (TEM) and selected area diffraction (SAD). Doppalapudi[5] *et. al.*, using TEM and SAD, found evidence for long-range atomic ordering as well as phase separation in MBE-grown $In_xGa_{1-x}N$ films. The driving force for the phase separation and atomic ordering is the 10% difference between the relaxed Ga-N and In-N bond lengths. Ho and Stringfellow[6] predicted the solid phase miscibility gap of $In_xGa_{1-x}N$ with a modified valence-force-field model.

The theoretical prediction, and confirming experimental observations, of phase separation in the $In_xGa_{1-x}N$ system suggests the following inter-related questions. First, how does the phase separation affect the optical properties of the material? Second, is there a non-destructive optical characterization method that can be used to detect the occurrence of phase separation? We address these questions by performing optical transmittance, Raman, and double spectrally resolved photoluminescence excitation (DSR-PLX) spectroscopy of MOCVD-grown $In_xGa_{1-x}N$ films with x=0.06 to x=0.49, that were previously analyzed[4] for phase separation. Each of these techniques is found to provide different information about the structure of the samples.

EXPERIMENT

$In_xGa_{1-x}N$ films were grown on (0001) sapphire substrates using a specially designed metal-organic chemical vapor deposition (MOCVD) reactor and growth conditions that have been described elsewhere (E.L. Piner[4] *et. al.* and references therein). An AlN buffer layer and then a AlGaN graded to GaN prelayer were grown on each substrate before the $In_xGa_{1-x}N$ layer; the $In_xGa_{1-x}N$ layer thickness is estimated to be 0.3 μm to 0.5 μm, and the AlGaN/GaN prelayer thickness is estimated to be 0.1 μm. The growth temperature for the $In_xGa_{1-x}N$ layer was between 690°C and 780°C. The In fraction, x, was controlled by varying the growth temperature and the hydrogen gas flow rate. Eleven films were examined, with x=0.06 to x=0.49 as determined from the shift of the 0002 XRD peak relative to pure GaN and InN, assuming a linear x-dependence of the lattice constant.

All optical measurements were performed at room temperature. Transmittance spectra of the samples were measured with a Cary model 14 spectrophotometer.[7] Metal-grid neutral density filters were inserted into the spectrophotometer reference channel to extend the lower end of the measured transmittance range to ~$3x10^{-5}$.

Raman spectra were excited by the 514.53 nm (2.409 eV) and 457.94 nm (2.707 eV) lines of an Argon ion laser and recorded by a Princeton Instruments intensified photodiode array detector attached to a Spex Triplemate monochromator.[7] The wavelength resolution of the monochromator was 0.10 nm, corresponding to a wavenumber resolution of 3.7 cm^{-1} for the Raman spectra excited at 514.53 nm, and 4.7 cm^{-1} for the Raman spectra excited at 457.94 nm. The wavenumber accuracy was ~0.2 cm^{-1}, calibrated with Ar, Kr and Xe line sources.

In the DSR-PLX experiment, PL was excited by a wavelength-tunable source, and the PL intensity within a selected wavelength band was monitored as the excitation energy was scanned. The measurement was then repeated for several different emission wavelength bands, so that several excitation spectra were obtained for each sample, corresponding to different emission wavelengths (or photon energies). The excitation source was a 300 watt xenon arc lamp coupled to a Spex model 1680 double monochromator.[7] The wavelength resolution of the spectrometer was 2 nm; the corresponding energy resolution varied from 0.006 eV at 1.9 eV, to 0.02 eV at 3.5 eV. Each emission band was selected by a bandpass interference filter, taken from a set of seven filters with center wavelengths every 50 nm from 450 nm to 750 nm and full bandwidths of 40 nm. To more completely remove the scattered excitation, each bandpass filter was paired with a longpass filter that had a cut-on wavelength slightly shorter than the bandpass center wavelength. The emitted PL was detected by a S20 type photomultiplier tube. The excitation source was mechanically chopped at 200 Hz, enabling lock-in detection of the PL signal.

The wavelength (or photon energy) dependence of the DSR-PLX source intensity was measured with a NIST-calibrated[8] silicon photodiode. By correcting for the wavelength dependence of the source intensity, the DSR-PLX spectra were normalized to a scale proportional to the number of emitted photons per exciting photon; the absolute quantum efficiency was not measured.

RESULTS AND DISCUSSION

Fig. 1 shows optical transmittance spectra of five samples, plotted on a semilog scale. For most of the samples, log(transmittance) decreases approximately linearly with energy above an absorption edge. The absorption edge energy decreases with increasing x. All the samples show a second absorption edge at 3.4 eV, the band gap of pure GaN. The 3.4 eV feature is attributed to the GaN prelayers. The x-dependence of the primary absorption edge energy is plotted in Fig. 2, together with a linear fit to the data. The x=0.06 and x=0.18 samples are not shown in Fig. 2 because their absorption edge energies could not be determined accurately due to the large widths of the edges. The x=0.49 sample is shown in Fig. 2, but is excluded from the

https://doi.org/10.1557/S1092578300002490 Published online by Cambridge University Press

linear fit because the absorption edge energy does not decrease from x=0.43 to x=0.49.

The band gap reported[9] for pure InN is 1.9 eV. It is thus surprising that the observed absorption edge of these samples reaches 1.9 eV at x=0.36, and decreases below 1.9 eV for the samples with x≥0.4. The unexpectedly large shift of the absorption edge with x for all samples (including those with x<0.2) can be compared with the previous SAD and TEM measurements, which showed spinodal decomposition only for x>0.2. We tentatively attribute the large absorption edge shift to compositional inhomogeneity on the cation sublattice, i.e. clustering of Ga and In atoms, although other defect structures such as nitrogen vacancies cannot be ruled out. The possible observation of inhomogeneity in the x<0.2 films by absorption spectroscopy, but not by SAD or TEM, suggests that absorption is sensitive to inhomogeneity on a shorter length scale than the other techniques.

Raman spectra of the x≥0.28 samples, obtained with 2.409 eV or 2.707 eV excitation, are shown in Fig. 3. (Raman spectra could not be observed for the x<0.28 samples because of strong interfering luminescence in the Raman region. The interfering luminescence was weaker in the x≥0.28 samples, and was subtracted from the spectra shown in Fig. 3 by a curve-fitting method.) The dominant component of these spectra is the A_1(LO) mode. For comparison, the A_1(LO) frequencies of pure GaN and InN are shown in Fig. 3 as dashed lines. The separation between the Raman peaks measured at the two excitation energies, as well as the width of each peak, is seen to increase with increasing x. To better display the trends in the data, the full widths at half maximum of the A_1(LO) peaks are plotted as functions of x in Fig. 4(a), and the separation between the centers of the peaks measured at the two excitation energies is plotted as a function of x in Fig. 4(b). The broadening with increasing x [Fig. 4(a)] is tentatively attributed to an increase in compositional inhomogeneity. The separation between the peaks [Fig. 4(b)] is tentatively attributed to selective excitation of portions of the inhomogeneous sample with different compositions, and different A_1(LO) frequencies, at each excitation energy. In the resonant Raman effect, the scattering intensity is enhanced when the incident photon energy is near the band gap. In our experiment, each excitation energy (2.409 eV and 2.707 eV) is equal to the $In_xGa_{1-x}N$ band gap for a specific composition $x(E_{exc})$; we thus suggest that the Raman intensity is enhanced from portions of the sample with $x \approx x(E_{exc})$.

DSR-PLX spectra were obtained from samples with x=0.06, x=0.19, x=0.28, x=0.36 and x=0.43. Each PLX spectrum has a sigmoidal shape: the excitation efficiency (number of emitted photons per excitation photon), denoted η, increases from a lower value η_{low} to a higher value η_{high} within a specific energy range. To characterize the PLX spectra in a simple way, we define the threshold energy E_0 as the energy corresponding to the midpoint of the increase in excitation efficiency, i.e. $\eta(E_0)=0.5(\eta_{low} + \eta_{high})$. A model function was fitted to the data to obtain values for E_0. DSR-PLX spectra from the x=0.06 and x=0.28 samples are shown in Figs. 5(a) and 5(b), where each DSR-PLX spectrum is labeled with the center photon energy of the detected emission band; the data are plotted as solid lines; the model functions are plotted as dashed lines; and the calculated E_0 are marked by open circles. The value of E_0 is almost independent of emission energy in the x=0.06 [Fig. 5(a)] and x=0.19 samples. In contrast, E_0 shifts by a large amount with emission energy in the x=0.28 [Fig. 5(b)], x=0.36, and x=0.43 samples.

The DSR-PLX results are summarized in Fig. 6, where E_0 is plotted as a function of emission energy for each of the five samples. The data show in Fig. 6 confirm that the samples fall into two groups; for x=0.06 and x=0.19, E_0 is almost independent of emission energy, but for x≥0.28, E_0 has a strong dependence on emission energy, decreasing by about 1 eV as the emission energy decreases from 2.73 eV to 1.90 eV. Note that the first group corresponds to the samples that appears to be single-phase (x<0.2), while the second group corresponds to the samples that appear to be phase-separated (x>0.2) by SAD and TEM.

Several features complicated the analysis of the DSR-PLX spectra. Firstly, many of the

https://doi.org/10.1557/S1092578300002490 Published online by Cambridge University Press

spectra could not be measured to low enough excitation energy to accurately determine η_{low}, and uncertainty in η_{low} leads to uncertainty in E_0. This uncertainty was taken into account in the error analysis (error bars on E_0 in Fig. 6). Secondly, several spectra contain a distinct peak between 2 eV and 2.5 eV. A peak in this region was also observed in PLX spectra of an uncoated sapphire substrate, shown in Fig. 5(c), and is thus attributed to impurity centers in the substrate. The substrate peak was subtracted as part of the data analysis used to determine E_0. Finally, a derivative-like feature near 2.9 eV occurs in several spectra; other measurements suggest that this feature is a instrumental artifact.

Although both Raman and DSR-PLX spectra appear to be sensitive to compositional inhomogeneity, there is an important difference between them. The Raman spectra vary noticeably with x in the higher-x samples (Fig. 4), while the DSR-PLX spectra show little change from x=0.28 to x=0.43 (Fig. 6). To explain these results, consider the physical properties examined by the two techniques. Raman scattering probes optical phonon frequencies, which are sensitive to intermediate-range (~10 nm) structural order. DSR-PLX, on the other hand, probes interband electronic transitions, which are determined mostly by short-range order. We suggest that the size of the phase-separated regions increases from x=0.28 to x=0.49, and this increase has a greater effect on the phonon frequencies (Raman) than on the interband electronic transitions (PLX). The previous TEM observations[4] support our hypothesis: TEM images showed a distinct "tweed" appearance, indicating spinodal decomposition on a relatively large length scale, for the x=0.49 sample, but not for the x=0.28 sample.

CONCLUSIONS

Transmittance, excitation-wavelength dependent Raman, and double spectrally resolved photoluminescence excitation (DSR-PLX) spectroscopies were used to characterize $In_xGa_{1-x}N$ films with x=0.06 to x=0.49. The transmittance data suggest that compositional inhomogeneity is present even in the lower-x samples (x<0.2), in which inhomogeneity was not detected by microstructural methods (TEM, SAD, and XRD). Both Raman and DSR-PLX show "spectral signatures" that correlate with compositional inhomogeneity and phase separation in the higher-x samples (x>0.2). The composition dependence of the Raman spectra, from x=0.28 to x=0.49, is consistent with an increase in the size of the phase-separated regions with increasing x. In contrast, the DSR-PLX spectra show little change from x=0.28 to x=0.43.

ACKNOWLEDGEMENTS

The work at North Carolina State University was supported by ONR (University Research Initiative) under grant N00014-92-J_1477 and ARO/ARPA under grant DAAH04-96-1-0173.

---

[1] L. Sugiura, J. Nishio, M. Onomura, S. Nunoue, K. Itaya, and M. Ishikawa, in *Nitride Semiconductors*, edited by F.A. Ponce, S.P. DenBaars, B.K. Meyer, S. Nakamura, and S. Strite (Mater. Res. Soc. Proc. 482, Warrendale, PA, 1998), p. 1157-1167
[2] K. Osamura, S. Naka, and Y. Murakami, J. Appl. Phys. **46**, 3432 (1975)
[3] R. Singh, D. Doppalapudi, T.D. Moustakas, and L.T. Romano, Appl. Phys. Lett. **70**, 1089 (1997)
[4] E.L. Piner, N.A. El-Masry, S.X. Liu and S.M. Bedair, in *Nitride Semiconductors,* ibid., p. 125-130
[5] D. Doppalapudi, S.N. Basu, K.F. Ludwig, Jr. and T.D. Moustakas, J. Appl. Phys. **84**, 1389 (1998)
[6] I. Ho and G.B. Stringfellow, Appl. Phys. Lett. **69**, 2701 (1996)
[7] The use of trade names or brand names does not imply endorsement of the product by NIST.
[8] T.C. Larason, S.S. Bruce and C. L. Cromer, J. Res. Natl. Inst. Stand. Technol. **101**, 133 (1996)
[9] S. Strite and H. Morkoc, J. Vac. Sci. Technol. B **10**, 1237 (1992)

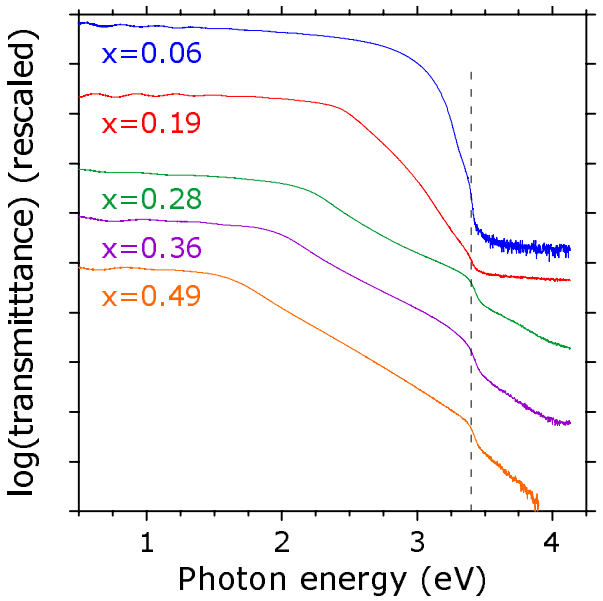

Fig. 1. Transmittance spectra of $In_xGa_{1-x}N$ samples with varying In fraction (x). Vertical line: GaN absorption edge at 3.4 eV.

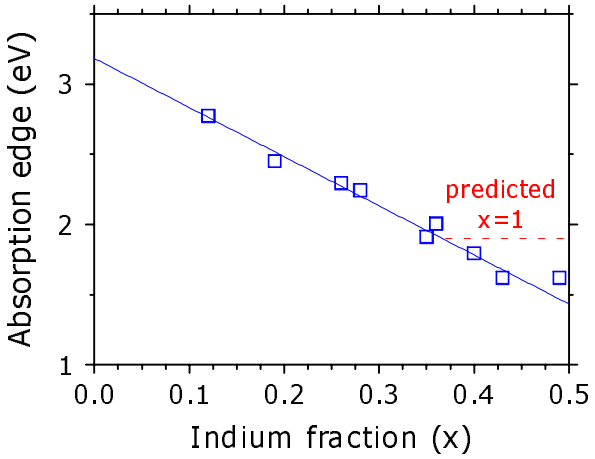

Fig. 2. Shift of absorption edge with In fraction. Solid line: best fit, excluding x=0.49. Dashed horizontal line: predicted absorption edge of pure InN (x=1).

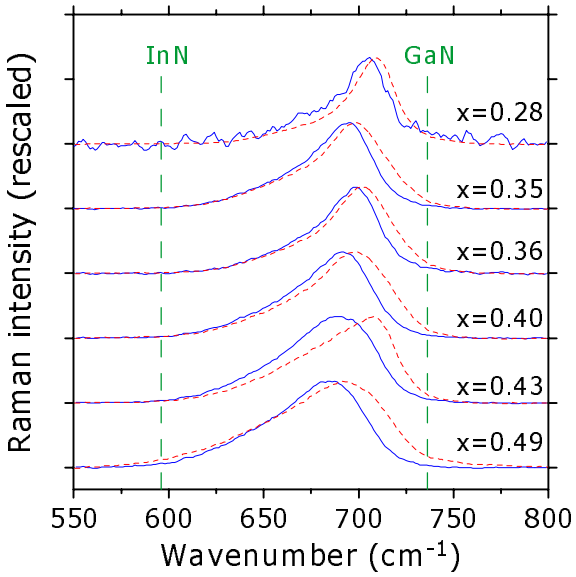

Fig. 3. Raman spectra of $In_xGa_{1-x}N$ samples. Solid lines: 2.409 eV excitation; dashed lines: 2.707 eV excitation; vertical dashed lines: A_1(LO) frequencies of pure InN and GaN.

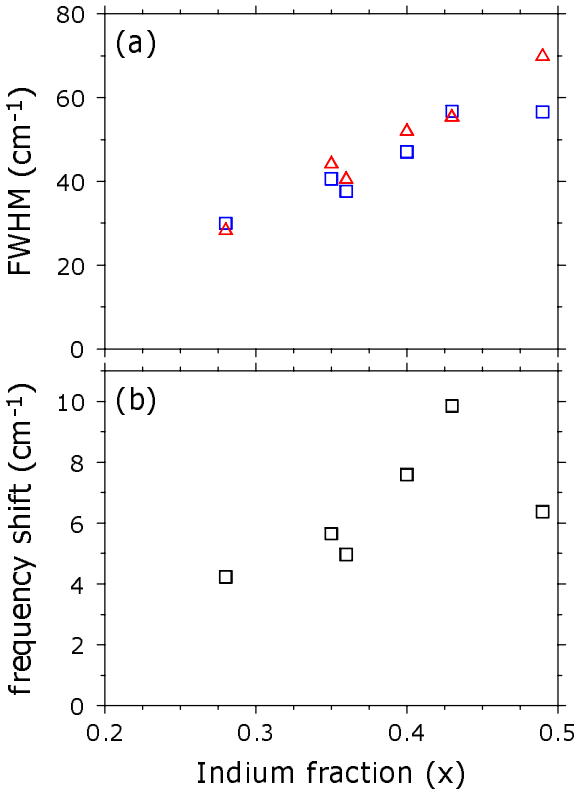

Fig. 4. x dependence of (a) FWHMs of Raman peaks excited at 2.409 eV (squares) and 2.707 eV (triangles); (b) separation between centers of Raman peaks excited at 2.409 eV and 2.707 eV.

https://doi.org/10.1557/S1092578300002490 Published online by Cambridge University Press

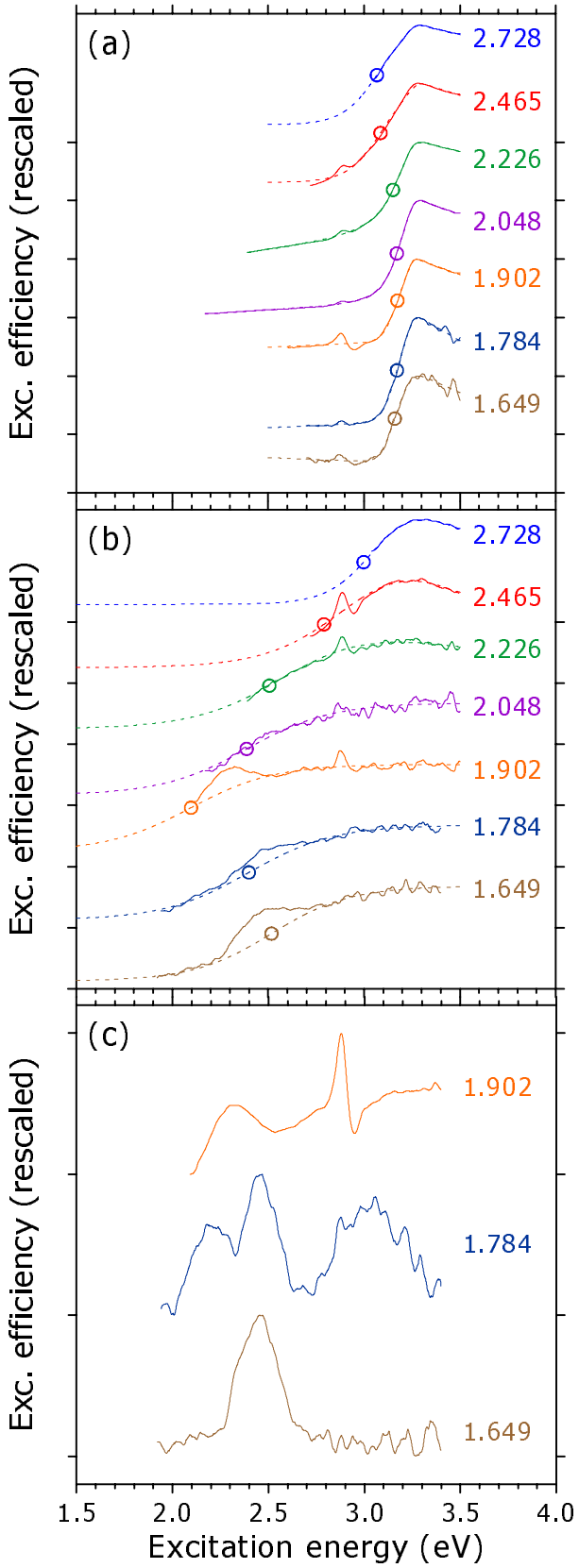

Fig. 5 (left). Double spectrally resolved photoluminescence excitation (DSR-PLX) spectra of (a) x=0.06 sample, (b) x=0.28 sample, and (c) sapphire substrate. For each spectrum, a label indicates the center of the detected emission energy band (eV), and the excitation threshold E_0 (midpoint of the transition from low to high excitation efficiency) is marked by an open circle.

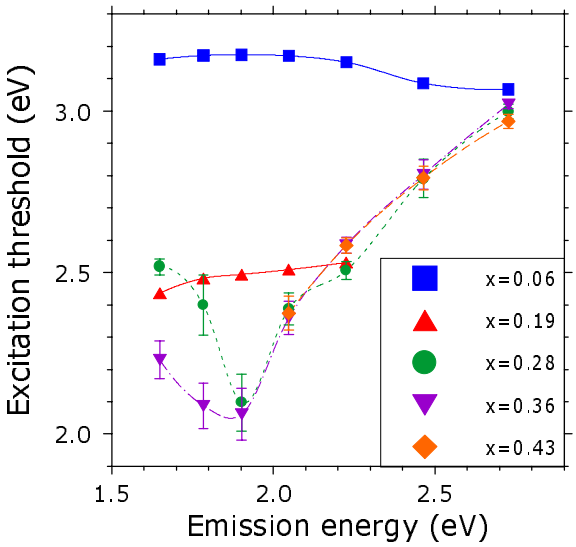

Fig. 6. Variation of excitation threshold energy of DSR-PLX spectra with emission energy, for five samples with differing In fractions (x). Interpolating curves that connect the data points have no theoretical significance.

https://doi.org/10.1557/S1092578300002490 Published online by Cambridge University Press